incorporation ($P = .85$), but was very different from the line for inhibition of [^{3}H]thymidine incorporation ($P < .0001$). From these data we conclude that the incorporation of [^{32}P]phosphate was a good measure of DNA synthesis in ribavirin-treated cells whereas the incorporation of [^{3}H]thymidine was not.

We also compared the foregoing data to the inhibitory effect of ribavirin on [^{3}H]dTTP formation. Data derived from Fig. 2 and from similar experiments at lower drug concentrations were regressed against log drug concentrations. The I_{50} concentration for inhibition of [^{3}H]dTTP formation interpolated from the dose-response line (Fig. 3) was 4.3 μM (2.7 to 6.8 μM). This dose-response line was similar to the line for inhibition of [^{3}H]thymidine incorporation into DNA ($P = .18$), but was significantly different from the lines for inhibition of [^{32}P]phosphate incorporation into DNA ($P < .0001$) and DNA fluorescence ($P < .0001$). On the basis of the similarity between effects of ribavirin on the incorporation of [^{3}H]thymidine into dTTP and DNA, we conclude that ribavirin has a potent effect on the labeling of dTTP and that this effect is primarily responsible for the inhibition of [^{3}H]thymidine incorporation into DNA. The marked inhibition by ribavirin of [^{3}H]thymidine incorporation in other primary (*1, 3, 4*) and established (*1, 5–7*) cell lines suggests the phenomenon extends to many types of mammalian cells.

Our data indicate that when DNA synthesis is measured by methods other than incorporation of [^{3}H]thymidine, ribavirin is a weak inhibitor in KB cells and human lymphocytes. The use of [^{3}H]thymidine to measure DNA synthesis is inaccurate because of the effect of ribavirin on [^{3}H]dTTP formation. These observations lead to the general premise that the sole use of [^{3}H]thymidine to measure DNA synthesis in drug-treated mammalian cells may cause serious misinterpretations of data.

JOHN C. DRACH
MARK A. THOMAS
JIMMY W. BARNETT
SANDRA H. SMITH
CHARLES SHIPMAN, JR.
Dental Research Institute, University of Michigan, Ann Arbor, 48109

References and Notes

1. R. W. Sidwell, J. H. Huffman, G. P. Khare, L. B. Allen, J. T. Witkowski, R. K. Robins, *Science* **177**, 705 (1972).
2. R. W. Sidwell, R. K. Robins, I. W. Hillyard, *Pharmacol. Ther.* **6**, 123 (1979).
3. E. De Clercq and M. Luczak, *Life Sci.* **17**, 187 (1975); D. L. Swallow, *Ann. N.Y. Acad. Sci.* **284**, 289 (1977).
4. N. L. Pushkarskaya, V. V. Dikiy, G. A. Galegov, *Vopr. Med. Khim.* **24**, 84 (1978).
5. J. C. Drach and C. Shipman, Jr., *Ann. N.Y. Acad. Sci.* **284**, 396 (1977).
6. A. Larsson, K. Stenberg, B. Öberg, *Antimicrob. Agents Chemother.* **13**, 154 (1978).
7. W. E. G. Müller, A. Maidhof, H. Taschner, R. K. Zahn, *Biochem. Pharmacol.* **26**, 1071 (1977); M. J. Browne, *Antimicrob. Agents Chemother.* **15**, 747 (1979).
8. D. G. Streeter, J. T. Witkowski, G. P. Khare, R. W. Sidwell, R. J. Bauer, R. K. Robins, L. N. Simon, *Proc. Natl. Acad. Sci. U.S.A.* **70**, 1174 (1973); B. Eriksson *et al.*, *Antimicrob. Agents Chemother.* **11**, 946 (1977); B. B. Goswami, E. Borek, O. K. Sharma, J. Fujitaki, R. A. Smith, *Biochem. Biophys. Res. Commun.* **89**, 830 (1979).
9. J. H. Huffman, R. W. Sidwell, G. P. Khare, J. T. Witkowski, L. B. Allen, R. K. Robins, *Antimicrob. Agents Chemother.* **3**, 235 (1973). In the present study, ribavirin also exhibited only limited cytotoxicity; the minimum inhibitory concentration measured microscopically was 200 to 400 μM.
10. D. E. Lopatin, F. L. Peebles, I. S. Horner, *Clin. Immunol. Immunopathol.* **16**, 75 (1980).
11. Relative amounts of DNA synthesized in each culture were determined in the following manner: (i) the area under the cytofluorometric histogram from each culture—including those held at 2°C and those without ribavirin—was summed and divided by 10,000 (the number of nuclei examined in each flow cytometer run) to give the average amount of DNA fluorescence per cell; (ii) this value was multiplied by the number of cells per culture to give the amount of DNA fluorescence per culture; and (iii) the average value obtained from the cultures held at 2°C was subtracted from values obtained from all other cultures. These final values represent the increase in DNA content which occurred in untreated and ribavirin-treated cultures during the incubation period.
12. Dose-response relationships were constructed by linearly regressing probit values of parameters related to DNA synthesis against log drug concentrations. The I_{50} concentrations and corresponding 95 percent confidence intervals were calculated from the regression lines by using methods described by A. Goldstein [*Biostatistics: An Introductory Text* (Macmillan, New York, 1964), pp. 156–161].
13. Identity of any two dose-response curves was tested by calculating P values for the equality of the regressions and slopes as described by D. J. Fox and K. E. Guire [*MIDAS: Michigan Interactive Data Analysis System* (Univ. of Michigan Press, Ann Arbor, 1973), pp. 59–60]. The slopes of the immediately adjacent dose-response curves compared in this study were similar ($P > .80$), consequently P values given in the text refer only to the comparison of regressions.
14. C. Shipman, Jr., *et al.*, *Antimicrob. Agents Chemother.* **9**, 120 (1976).
15. C. Shipman, Jr., *Proc. Soc. Exp. Biol. Med.* **130**, 305 (1969).
16. P. M. Schwartz and J. C. Drach, *J. Chromatog.* **106**, 200 (1975).
17. J. C. Drach, J. N. Sandberg, C. Shipman, Jr., *J. Dent. Res.* **56**, 275 (1977).
18. A. Krishan, *J. Cell Biol.* **66**, 188 (1975).
19. We thank D. E. Lopatin for providing lymphocytes and guidance in their experimental use. We also thank W. D. Ensminger for valuable discussions and use of the flow cytometer. This work was supported by PHS grant DE 02731 from the National Institute of Dental Research.

6 August 1980; revised 24 November 1980

Ctenidial Autotomy in *Corbicula fluminea* in Response to Massive Granulomas

Abstract. *Large granulomas (greater than 2 millimeters in diameter), stimulated by the presence of and formed around necrotic larval tissue in the inner demibranchs of* Corbicula fluminea, *are eliminated by autotomy. Granulocytes invade and destroy ctenidial epithelium adjacent to the granuloma, causing it and the granuloma to slough away into the mantle cavity, where they are removed as pseudofeces.*

Foreign material in the bodies of mollusks has been found to elicit one of three kinds of cellular defense mechanisms: phagocytosis, encapsulation, or nacrezation (*1*). We report here a fourth defense mechanism, autotomy, which is induced by the presence of massive hyperplasic granulomas encapsulating necrotic larval tissue in ctenidial (gill) marsupia of the bivalve *Corbicula fluminea* (Müller 1774). Morton (*2*) described the development of granulomas in the ctenidial marsupium of *C. fluminea* from Plover Cove, Hong Kong. Like many freshwater bivalves, *C. fluminea* retains the larvae within the ctenidia (inner demibranchs) before releasing them into the environment. Occasionally some larvae die while in the marsupium. If dead larvae are not moved from the ctenidial marsupia to the exterior via the suprabranchial chamber and excurrent siphon, they are encapsulated by epithelioid cells and cyst-associated granulocytes. Morton (*2*) described in detail the process of granuloma formation and concluded that amoebocytes "probably reabsorb the larval cellular debris." We have observed *C. fluminea* from several localities in California and Texas which bear similar larvae-induced ctenidial granulomas. At least some are removed, not by the activities of phagocytes, but by autotomy of the affected tissue.

We found that the incidence of ctenidial granulomas is closely correlated with clam size (Fig. 1a) and reproductive periodicity (Fig. 1, b and c) (*3*). Clams with shells longer than 30 mm frequently contain cysts up to 5 mm in diameter after the spring and fall peaks of larvae production. About 1 month after the appearance of the large granulomas, approximately 40 to 50 percent of the affected clams have torn, ragged inner demibranchs and few, if any, large granulomas (Fig. 1c). We observed material as large as 3 by 4 mm (subsequently identified as fragments of ctenidial tissue surrounding granulomas) expelled as pseudofeces from the mantle cavity through the incurrent siphon. Ctenidia examined at periodic intervals for 6 months after the loss of granulomas show progressive tissue repair, with eventual restoration of normal ctenidial size (Fig. 1c).

0036-8075/81/0501-0551$00.50/0

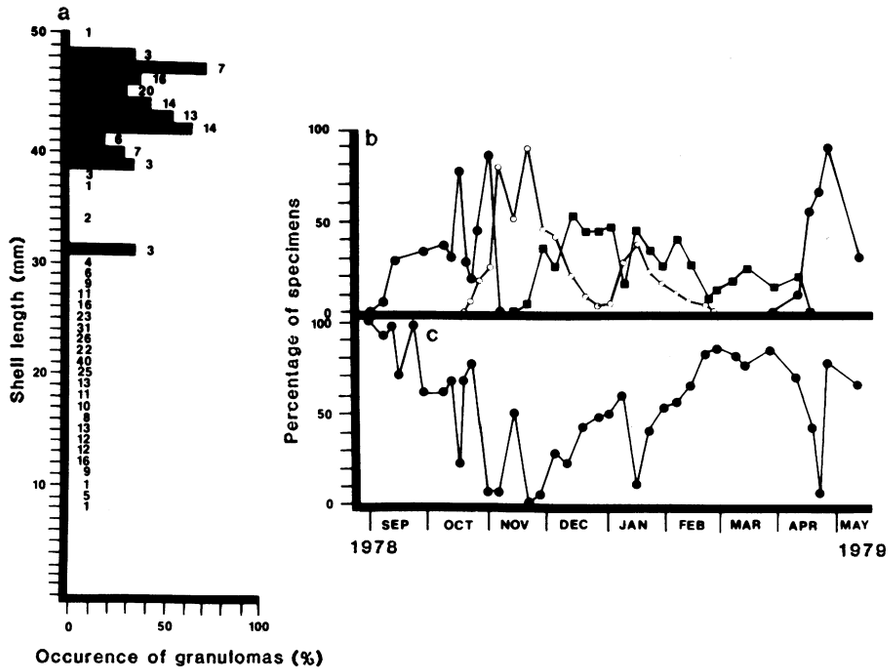

Fig. 1. (a) Incidence of larva-induced granulomas (percentage of organisms dissected) in *C. fluminea* of different sizes. The number of specimens examined in each size class is given beside the bars. The animals were collected on 5 November 1978. (b) Percentage of specimens > 30 mm (*N* as above) with inner demibranchs bearing embryos or larvae (●), with massive (> 2 mm in diameter) larva-induced granulomas (○, or with torn or ragged inner demibranchs (■) in which more than one-fifth of the structure was lost. (c) Percentage of specimens > 30 mm ($N = 10$ for each 38 sampling periods) bearing normal nonincubatory ctenidia. These specimens contained no developmental or larval stages or larva-induced granulomas in their inner demibranchs; the ctenidia were intact. Totals exceed 100 percent because some specimens harbored more than one condition. Note the sequential occurrence of incubated larvae, granulomas, and torn demibranchs. All specimens were collected from Lake Benbrook, Tarrant County, Texas.

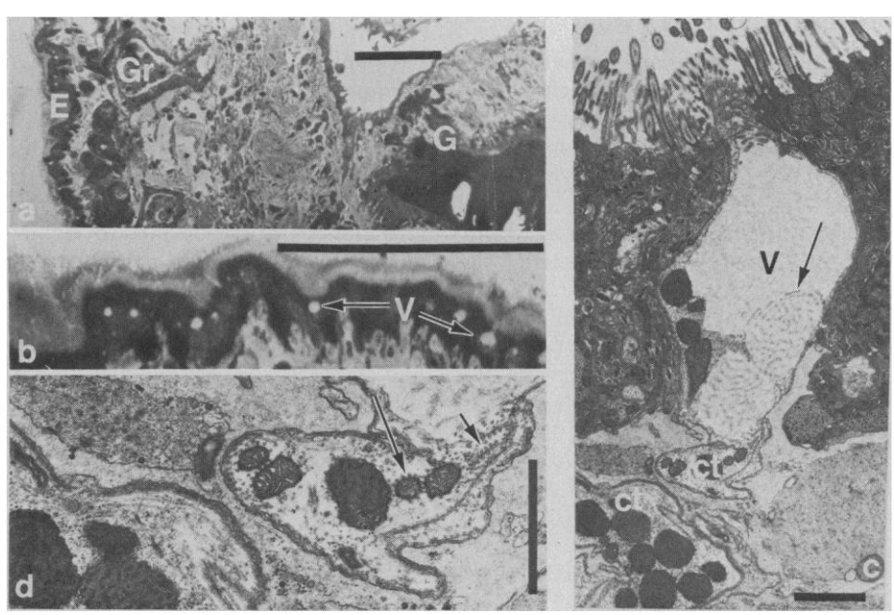

Fig. 2. (a) Light micrograph of massive granuloma (*G*) adjacent to ctenidial epithelium (*E*) being invaded by granulocytes (*Gr*). (b) Light micrograph of ctenidial epithelium containing cytoplasmic tubes and vacuolations (*V*) produced by invasive granulocytes. (c) Electron micrograph of cytoplasmic tubes (*ct*) and vacuolations produced by granulocytes in ctenidial epithelium. Note the disruption and expulsion of granule material (arrow) from granulocyte to extracellular space or vacuolated area. (d) Electron micrograph of cytoplasmic tubular area in (c) at site of degranulation. Note the arrays of microtubules at the periphery of the tube, conjoined to endoplasmic reticulum (short arrow) and encompassing mitochondria (long arrow). Scale bars: (a) and (b), 0.5 mm; (c) and (d), 1.0 μm.

In autotomy of ctenidial granulomas, granulocytes invade ctenidial epithelium in areas not directly associated with granuloma hyperplasia. We prepared four clams with ctenidial granulomas for electron microscopy. Tissue specimens were fixed in 3 percent glutaraldehyde (which was dissolved in 0.1*M* Sorenson's phosphate buffer at *p*H 7.4), postfixed in 1 percent OsO_4 in the same buffer, dehydrated, and embedded in Spurr's low-viscosity medium. Thick sections (2.0 μm) were cut and stained with methylene blue and Azur II. Thin sections (~ 100 nm) were also made from the same blocks and stained with uranyl acetate and lead citrate.

Examination of these sections suggested the following sequence of events. Adjacent to areas of massive granulomas, granulocytes appear in ctenidial blood sinuses, where they begin to disrupt or destroy ctenidial filaments and epithelia (Fig. 2, a and b). The granulocytes did not resemble any previously described bivalve hemocyte (*4*) or any of the granulocytes or other cells associated with the massive granulomas. Large aggregates of these granulocytes occupy filamentary blood sinuses and thereby gain access to adjacent ctenidial connective tissue and epithelia. The granulocytes invade the area of filamentary connective tissue supports, destroying the connective tissue matrix—apparently by release of extracellular digestive enzymes from cytoplasmic granules. Before the invasion of the ctenidial filament by granulocytes, the normal plications (folds) of the ctenidium are greatly stretched by the enlarging granuloma. Upon disruption or destruction of the connective tissue supports by the invasive granulocytes, the last remnants of normal surficial plication in the affected portion of the ctenidium are lost. Subsequently (or concurrently with the attack on the connective tissue), granulocytes invade the epithelium by extending long cytoplasmic tubes into the epithelial layer (Fig. 2c). In cross section, these tubes resemble vacuoles. At the periphery of these tubes are highly ordered arrays of microtubules (Fig. 2d), which probably serve as cytoskeletal elements aiding motility (*5*). Microtubules are also found in conjunction with cytoplasmic membranes (probably endoplasmic reticulum), and they encompass mitochondria in an arrangement (Fig. 2d) similar to that observed in the axons of nerve cells (*6*). As the cytoplasmic tubes invade the epithelium, granules undergo ultrastructural alterations, expanding and probably releasing digestive enzymes. The secretions apparently are delivered into

epithelial tissues, dissolving pathways toward the epithelial surface (Fig. 2d). Viewed under light microscopy at this stage, the epithelium appears vacuolated; the connective tissue supports of the gill filaments have been largely destroyed and normal filamentary plications have disappeared (Fig. 2, a and b).

Ultimately, multiple pathways are digested through the epithelium to the ctenidial surface, with the result that the activity of the granulocytes reduces the integrity of the ctenidial epithelium suprajacent to the massive granuloma. Eventually the weight of the granuloma overcomes the weakened adjacent tissues and it detaches along with associated ctenidial tissue and is sloughed away and eliminated from the mantle cavity as pseudofeces.

Autotomy is uncommon among the Mollusca, and we know of no other instance whereby a neoplasm is naturally excised from affected tissue. The process described here represents a unique adaptation by a bivalve mollusk to eliminate a hyperplasic granuloma. This appears to be a gerontological phenomenon, because the inner demibranchs of clams with shells shorter than 30 mm are rarely observed to be torn. Thus Morton's (*2*) contention of reabsorption of the necrotic tissue may be correct for small clams. Only when the involvement becomes so large as to endanger normal ctenidial function or when clams become old (or large) is the radical step of tissue autotomy taken.

JOSEPH C. BRITTON
WAYNE J. BARCELLONA
JOHN HAGAN
MARK L. LAGRONE
Department of Biology, Texas Christian University, Fort Worth 76129

References and Notes

1. E. A. Malek and T. C. Cheng, *Medical and Economic Malacology* (Academic Press, New York, 1974), p. 191.
2. B. Morton, *J. Invertebr. Pathol.* **30**, 5 (1977).
3. That Morton (*2*) failed to observe the process described here may be explained in part by differences in the size of individual clams in Hong Kong and North America. *Corbicula fluminea* generally does not exceed 30 mm (shell length) in Plover Cove, Hong Kong; it frequently grows to 50 mm or more in many parts of the present North American distribution. Thus, autotomy of large granulomas may be gerontologically induced. Asian specimens may not normally live to the age or attain the body size at which massive granulomas form.
4. R. S. Anderson and R. A. Good, *J. Invertebr. Pathol.* **27**, 57 (1976); R. A. Baker, *ibid.*, p. 371; D. P. Cheney, *Biol. Bull. (Woods Hole, Mass.)* **140**, 353 (1971); D. S. Dundee, *Trans. Am. Microsc. Soc.* **72**, 254 (1953); A. S. Narain, *J. Morphol.* **137**, 63 (1972); *Malacol. Rev.* **6**, 1 (1973); M. R. Tripp, *Ann. N.Y. Acad. Sci.* **113**, 467 (1963).
5. P. Dustin, *Microtubules* (Springer-Verlag, New York, 1978), pp. 244–245, 264–272, and 295–296.
6. D. S. Smith, V. Järlfors, B. F. Cameron, *Ann. N.Y. Acad. Sci.* **253**, 472 (1975).
7. Supported by Office of Naval Research contract N00014-76-C-0897.

29 October 1980; revised 19 January 1981

Purified Reduced Nicotinamide Adenine Dinucleotide: Responses to Lactate Dehydrogenase Isozymes from Three Cell Sources

Abstract. *Lactate dehydrogenase (LDH, E.C. 1.1.1.27) isozymes from three single-cell sources reacted differently with reduced nicotinamide adenine dinucleotide (NADH) purified to published chromatographic and spectrophotometric specifications and free of inhibitors of LDH, when compared with a commercial preparation of NADH. The activity of LDH-1, purified from rabbit erythrocytes, increased the most with inhibitor-free NADH; the next most stimulated were the LDH isozymes from a control hepatocyte line; but hardly responsive at all were the same isozymes from chemically transformed cells. Thus isozyme composition alone did not account for the range of responses to purified NADH. The commercial preparation of NADH used in these studies contains the Strandjörd-Clayson inhibitors, the most potent group identified in NADH preparations relative to LDH activity. The results suggest that specific molecular differences in individual isozymes contribute to the differential response to the Strandjörd-Clayson inhibitors.*

Although reduced nicotinamide adenine dinucleotide (NADH) is required for catalytic activity by over 200 dehydrogenases of plant and animal origin (*1*), it is recognized that commercial preparations of the reductant contain variable amounts of contaminants (*2–4*) known to inhibit at least six dehydrogenases (*5*), as well as individual isozymes of LDH (*6*, *7*). Until now, investigators have not had the opportunity to study dehydrogenases with NADH purified to chromatographic and spectrophotometric specifications and free of inhibitors. Availability of such a preparation (*8*) encouraged the evaluation of steady-state activities compared with a commercial preparation of NADH.

For these studies, we selected three examples of LDH isozymes isolated from single-cell mammalian sources in order to eliminate isozyme contributions from different cell types present in intact organs. The enzymes are LDH-1, purified from rabbit erythrocytes (*9*), and two preparations from cell lines of rat hepatic origin, one a control line, TRL 12(13) (*10*), and one, NMU-3, transformed in vitro with nitrosomethylurea (*11*). Although the cells of hepatic origin cannot be distinguished by light microscopy, the NMU-3 line produces carcinomas in vivo. Both these lines are characterized by LDH-4 and -5, permitting comparison of the response to purified NADH with the same isozymes of related cell origin.

The activity of the LDH isozymes was determined by the method of Schwartz and Bodansky (*12*) with two preparations of NADH: NADH(A), Boehringer Mannheim, grade I, purchased through regular supply channels and stored over desiccant at 2°C, and NADH(B), purified by the same firm to meet chromatographic and spectrophotometric specifications for inhibitor-free material (*8*), sealed under nitrogen and stored at −20°C. Both samples were protected from light.

The results of these analyses are given in Table 1. The coefficient of variation of the enzyme assays was of the order of 0.7 percent, implying high reproducibility of these results (*13*). The activity of

Table 1. The activity of LDH preparations with NADH(A) and NADH(B).

LDH activity (IU/ml-min)*		Percentage difference (B)/(A) × 100
NADH(A)	NADH(B)	
LDH-1, erythrocytes		
203 ± 1.00	236 ± 2.00	16.26
189 ± 1.00	224 ± 0.00	18.52
Mean		17.39
Control hepatocytes		
282 ± 0.00	304 ± 6.00	7.80
300 ± 0.00	334 ± 6.00	11.33
225 ± 3.00	240 ± 0.00	6.67
242 ± 0.00	262 ± 0.00	8.26
Mean		8.52
Chemically transformed hepatocytes		
225 ± 3.00	229 ± 1.00	1.78
208 ± 2.00	214 ± 2.00	2.89
205 ± 1.00	208 ± 0.00	1.46
270 ± 2.00	278 ± 8.00	2.96
244 ± 0.00	256 ± 2.00	4.92
255 ± 3.00	257 ± 1.00	0.78
Mean		2.47

* Values represent the mean and standard deviation.

Table 2. Chromatographic analysis of NADH-(A) and NADH(B). The results are given as percentages of the total area of the chromatographic peaks at 254 nm (see Fig. 1).

Component	NADH(A)	NADH(B)
NADH	93.6	99.08
NAD^+	2.8	0.53
AMP	0.1	0.16
ADP-ribose	0.5	0.12
ADP	0.8	0.11
Nicotinamide	0.5	0
NMN	0.6	0
Peak 2 (Fig. 1)	0.4	0
Peak 1 (Fig. 1)	0.1	0

0036-8075/81/0501-0553$00.50/0